

# INVERSE ENTROPIC OPTIMAL TRANSPORT SOLVES SEMI-SUPERVISED LEARNING VIA DATA LIKELIHOOD MAXIMIZATION

**Mikhail Pershianov**

Skolkovo Institute of Science and Technology  
Moscow, Russia  
m.pershianov@skoltech.ru

**Arip Asadulaev**

Artificial Intelligence Research Institute  
ITMO University  
Moscow, Russia  
aripasadulaev@itmo.ru

**Nikita Andreev**

Independent Researcher  
Moscow, Russia  
nickmandreev@gmail.com

**Nikita Starodubcev**

Yandex Research  
Moscow, Russia  
nstarodubtsev@hse.ru

**Dmitry Baranchuk**

Yandex Research  
Moscow, Russia  
dbaranchuk@yandex-team.ru

**Anastasis Kratsios**

Vector Institute  
McMaster University  
Ontario, Canada  
kratsioa@mcmaster.ca

**Evgeny Burnaev & Alexander Korotin**

Skolkovo Institute of Science and Technology  
Artificial Intelligence Research Institute  
Moscow, Russia  
{e.burnaev, a.korotin}@skoltech.ru

## ABSTRACT

Learning conditional distributions  $\pi^*(\cdot|x)$  is a central problem in machine learning, which is typically approached via supervised methods with paired data  $(x, y) \sim \pi^*$ . However, acquiring paired data samples is often challenging, especially in problems such as domain translation. This necessitates the development of *semi-supervised* models that utilize both limited paired data and additional unpaired i.i.d. samples  $x \sim \pi_x^*$  and  $y \sim \pi_y^*$  from the marginal distributions. The usage of such combined data is complex and often relies on heuristic approaches. To tackle this issue, we propose a new learning paradigm that integrates both paired and unpaired data **seamlessly** through the data likelihood maximization techniques. We demonstrate that our approach also connects intriguingly with inverse entropic optimal transport (OT). This finding allows us to apply recent advances in computational OT to establish a **light** learning algorithm to get  $\pi^*(\cdot|x)$ . Furthermore, we demonstrate through empirical tests that our method effectively learns conditional distributions using paired and unpaired data simultaneously.

## 1 INTRODUCTION

Recovering conditional distributions  $\pi^*(y|x)$  from data is one of the fundamental problems in machine learning, which appears both in predictive and generative modeling. In predictive modeling, the standard examples of such tasks are the classification, where  $x \in \mathbb{R}^{D_x}$  is a feature vector and  $y \in \{0, 1, \dots, K\}$  is a class label, and regression, in which case  $x$  is also a feature vector and  $y \in \mathbb{R}^D$  is a real number. In generative modeling, both  $x$  and  $y$  are feature vectors in  $\mathbb{R}^{D_x}, \mathbb{R}^{D_y}$ , respectively, representing complex objects, and the goal is to find a transformation between them.

In our paper, we focus on the case when  $x$  and  $y$  are multi-dimensional real-value vectors and the true joint data distribution  $\pi^*(x, y)$  is a continuous data distribution on  $\mathbb{R}^{D_x} \times \mathbb{R}^{D_y}$ , i.e., we exclude the problems when, e.g.,  $y$  is a discrete object such as the class label. That is, the scope of our paper is the multi-dimensional probabilistic regression problems, which can be referred to as **domain translation** problems, as usually  $x$  and  $y$  are feature vectors representing data from different domains. In turn, the goal is to make a (probabilistic) prediction, where for a new object  $x_{new}$  from the input domain, we aim to predict the corresponding data  $y(x_{new})$  from the target domain, according to the conditional distribution  $\pi^*(y|x)$ .

It is very natural that to learn the conditional distributions  $\pi^*(y|x)$  of data one requires input-target data pairs  $(x, y) \sim \pi^*$ , where  $\pi^*$  is the true joint distribution of data. In this case,  $\pi^*(y|x)$  can be modeled via standard supervised learning approaches starting from a simple regression and ending with conditional generative models (Mirza & Osindero, 2014; Winkler et al., 2019). However, acquiring paired data may be costly, while getting unpaired samples  $x \sim \pi_x^*$  or  $y \sim \pi_y^*$  from two domains may be much easier and cheaper. This fact inspired the development of unsupervised (or unpaired) learning methods, e.g., (Zhu et al., 2017; Wu et al., 2020) among many others, which aim to somehow reconstruct the dependencies  $\pi^*(y|x)$  with access to unpaired data only.

While both paired (supervised) and unpaired (unsupervised) domain translation approaches are being extremely well developed nowadays, surprisingly, the semi-supervised setup when **both** paired and unpaired data is available is much less explored. This is due to the **challenge of designing learning objective** (loss) which can simultaneously take into account both paired and unpaired data. For example, one potential strategy here is to heuristically combine typical paired and unpaired losses. However, such a strategy leads to complex training objectives, see (Tripathy et al., 2019, §3.5), (Jin et al., 2019, §3.3), (Yang & Chen, 2020, §C), (Vasluianu et al., 2021, §3), (Panda et al., 2023, Eq. 8), (Tang et al., 2024, Eq. 8). Therefore, it is reasonable to raise a question: *is it possible to design a simple loss to learn  $\pi^*(y|x)$  which naturally takes into account both paired and unpaired data?*

**Contributions.** In our paper, we positively answer the above-raised question. Namely,

1. We introduce a novel loss function (optimization objective) designed to facilitate the learning of conditional distributions  $\pi^*(\cdot|x)$  using both paired and unpaired training samples derived from  $\pi^*$  (§3.1). This loss function is based on the well-established principle of likelihood maximization. Our approach’s notable advantage lies in its capacity to support end-to-end learning, thereby *seamlessly* integrating both paired and unpaired data into the training process.
2. We demonstrate the theoretical equivalence between our proposed loss function and the *inverse entropic optimal transport* problem (§3.2). This finding enables to leverage established computational OT methods to address challenges encountered in semi-supervised learning.
3. Building upon recent advancements in the field of computational optimal transport, we provide a *light* and *end-to-end* algorithm exploiting the Gaussian mixture parameterization specifically tailored to optimize our proposed likelihood-based loss function (in §3.3).

Our empirical validation in §5 shows the impact of both unpaired and paired data on overall performance. In particular, our findings reveal that conditional distributions  $\pi^*(\cdot|x)$  can be effectively learned even with a modest quantity of paired data  $(x, y) \sim \pi^*$ , provided that a sufficient amount of auxiliary unpaired data  $x \sim \pi_x^*, y \sim \pi_y^*$  is available.

**Notations.** Throughout the paper,  $\mathcal{X}$  and  $\mathcal{Y}$  represent Euclidean spaces, equipped with the standard norm  $\|\cdot\|$ , induced by the inner product  $\langle \cdot, \cdot \rangle$ , i.e.,  $\mathcal{X} \stackrel{\text{def}}{=} \mathbb{R}^{D_x}$  and  $\mathcal{Y} \stackrel{\text{def}}{=} \mathbb{R}^{D_y}$ . The set of absolutely continuous probability distributions on  $\mathcal{X}$  is denoted by  $\mathcal{P}_{\text{ac}}(\mathcal{X})$ . For simplicity, we use the same notation for both the distributions and their corresponding probability density functions. The joint probability distribution over  $\mathcal{X} \times \mathcal{Y}$  is denoted by  $\pi$  with corresponding marginals  $\pi_x$  and  $\pi_y$ . The set of joint distributions with given marginals  $\alpha$  and  $\beta$  is represented by  $\Pi(\alpha, \beta)$ . We use  $\pi(\cdot|x)$  for the conditional distribution, while  $\pi(y|x)$  represents the conditional density at a specific point  $y$ . The differential entropy is given by  $H(\beta) = - \int_{\mathcal{Y}} \beta(y) \log \beta(y) dy$ .

## 2 BACKGROUND

First, we recall the formulation of the domain translation problem (§2.1). We remind the difference between its paired, unpaired, and semi-supervised setups. Next, we recall the basic concepts of the inverse entropic optimal transport, which are relevant to our paper (§2.2).

### 2.1 DOMAIN TRANSLATION PROBLEMS

The goal of *domain translation* (DT) task is to transform data samples from the source domain to the target domain while maintaining the essential content or structure. This approach is widely used in applications like computer vision (Zhu et al., 2017; Lin et al., 2018; Peng et al., 2023), natural language processing (Jiang et al., 2021; Morishita et al., 2022), and audio processing (Du et al., 2022), etc. Domain translation task setups can be classified into supervised (or paired), unsupervised (or unpaired), and semi-supervised approaches based on the data used for training (see Figure 1).

**Supervised (Paired) Domain Translation** relies on matched examples from both the source and target domains, where each input corresponds to a specific output, enabling direct supervision during the learning process. Formally, this setup assumes access to a set of  $P$  empirical pairs  $XY_{\text{paired}} \stackrel{\text{def}}{=} \{(x_1, y_1), \dots, (x_P, y_P)\} \sim \pi^*$  from some unknown joint distribution. The goal here is to recover the conditional distributions  $\pi^*(\cdot|x)$  to generate samples  $y|x_{\text{new}}$  for new inputs  $x_{\text{new}}$  that are not present in the training data. While this task is relatively straightforward to solve, obtaining such paired training datasets can be challenging, as it often involves significant time, cost, and effort.

**Unsupervised (Unpaired) Domain Translation**, in contrast, does not require direct correspondences between the source and target domains (Zhu et al., 2017, Figure 2). Instead, it involves learning to translate between domains using unpaired data, which offers greater flexibility but demands advanced techniques to achieve accurate translation. Formally, we are given  $Q$  unpaired empirical samples  $X_{\text{unpaired}} \stackrel{\text{def}}{=} \{x_1, \dots, x_Q\} \sim \pi_x^*$  from the source distribution and  $R$  unpaired samples  $Y_{\text{unpaired}} \stackrel{\text{def}}{=} \{y_1, \dots, y_R\} \sim \pi_y^*$  from the target distribution. Our objective is to learn the conditional distributions  $\pi^*(\cdot|x)$  of the unknown joint distribution  $\pi^*$ , whose marginals are  $\pi_x^*, \pi_y^*$ , respectively. Clearly, the primary challenge in unpaired setup is that the task is inherently ill-posed, leading to multiple potential solutions, many of which may be ambiguous or even not meaningful (Moriakov et al., 2020). Ensuring the translation’s accuracy and relevance requires careful consideration of constraints and regularization strategies to guide the learning process (Yuan et al., 2018). Overall, the unpaired setup is very important because of large amounts of unpaired data in the wild.

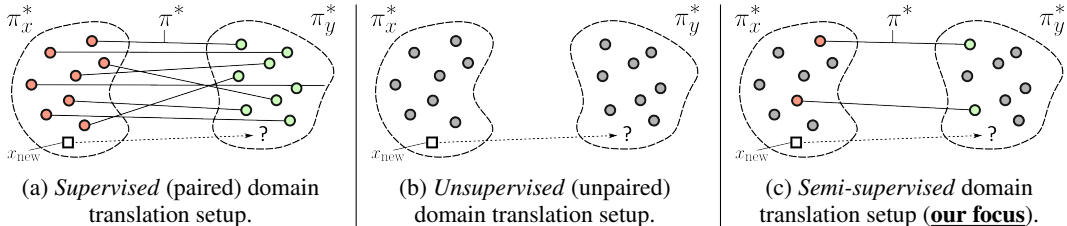


Figure 1: Visualization of domain translation setups. Red and green colors indicated paired training data  $XY_{\text{paired}}$ , while grey color indicates the unpaired training data  $X_{\text{unpaired}}, Y_{\text{unpaired}}$ .

**Semi-supervised domain translation** combines both approaches by utilizing a mix of paired and unpaired data (Tripathy et al., 2019; Jiang et al., 2023). This setup aims to leverage the advantages of paired data to guide the translation process while also taking advantage of the larger volume of unpaired data to improve the model’s performance and generalization. Formally, one assumes access to both pairs  $XY_{\text{paired}} \sim \pi^*$  and additional unpaired samples  $X_{\text{unpaired}} \sim \pi_x^*, Y_{\text{unpaired}} \sim \pi_y^*$ . Note that since paired samples can also be used in the unpaired manner, by convention, we assume that  $P \leq Q, R$  and first  $P$  unpaired samples are exactly the paired ones, i.e.,  $x'_r = x_r$  and  $y'_r = y_r$  for  $r \leq P$ . In turn, the goal is still to learn  $\pi^*(\cdot|x)$  using the available samples.

## 2.2 OPTIMAL TRANSPORT (OT)

The foundations of optimal transport (OT) are detailed in the seminal book by (Villani et al., 2009). For a more comprehensive overview, we refer to (Santambrogio, 2015; Peyré et al., 2019).

**Entropic OT** (Cuturi, 2013; Genevay, 2019). Consider source  $\alpha \in \mathcal{P}_{\text{ac}}(\mathcal{X})$  and target  $\beta \in \mathcal{P}_{\text{ac}}(\mathcal{Y})$  distributions. Let  $c^* : \mathcal{X} \times \mathcal{Y} \rightarrow \mathbb{R}$  be a cost function. The *entropic* optimal transport problem between distributions  $\alpha$  and  $\beta$  is then defined as follows:

$$\text{OT}_{c^*, \varepsilon}(\alpha, \beta) \stackrel{\text{def}}{=} \min_{\pi \in \Pi(\alpha, \beta)} \mathbb{E}_{x, y \sim \pi} [c^*(x, y)] - \varepsilon \mathbb{E}_{x \sim \alpha} \text{H}(\pi(\cdot|x)), \quad (1)$$

where  $\varepsilon > 0$  is the regularization parameter. Setting  $\varepsilon = 0$  recovers the classic OT formulation (Villani et al., 2009) originally proposed by (Kantorovich, 1942). With mild assumptions, the transport plan  $\pi^* \in \Pi(\alpha, \beta)$  that minimizes the objective (1) exists uniquely. It is called the *entropic OT plan*.

We note that in the literature, the entropy regularization term in (1) is usually  $-\varepsilon \text{H}(\pi)$  or  $+\varepsilon \text{KL}(\pi || \alpha \times \beta)$ . However, these forms are equivalent up to constants, see discussion in (Mokrov et al., 2024, §2) or (Gushchin et al., 2023, §1). In our paper, we work only with formulation (1), which is also known as the *weak* form of the entropic OT, see (Gozlan et al., 2017; Backhoff-Veraguas et al., 2019; Backhoff-Veraguas & Pammer, 2022).

**Dual formulation.** With mild assumptions on  $c^*, \alpha, \beta$ , the following dual OT formulation holds:

$$\text{OT}_{c^*, \varepsilon}(\alpha, \beta) = \sup_f \left\{ \mathbb{E}_{x \sim \alpha} f^{c^*}(x) + \mathbb{E}_{y \sim \beta} f(y), \right\} \quad (2)$$

where  $f$  ranges over a certain subset of continuous functions (dual potentials) with mild assumptions on their boundness, see (Backhoff-Veraguas & Pammer, 2022, Eq. 3.3) for details. The term  $f^{c^*}$  represents the so-called *weak entropic  $c^*$ -transform* of  $f$ , defined as:

$$f^{c^*}(x) \stackrel{\text{def}}{=} \min_{\beta \in \mathcal{P}(\mathcal{Y})} \left\{ \mathbb{E}_{y \sim \beta} [c^*(x, y)] - \varepsilon \text{H}(\beta) - \mathbb{E}_{y \sim \beta} f(y) \right\}. \quad (3)$$

It has closed-form (Mokrov et al., 2024, Eq. 14), which is given by

$$f^{c^*}(x) = -\varepsilon \log \int_{\mathcal{Y}} \exp \left( \frac{f(y) - c^*(x, y)}{\varepsilon} \right) dy. \quad (4)$$

**Inverse entropic OT.** The forward OT problem (1) focuses on determining the OT plan  $\pi^*$  given a predefined cost function  $c^*$ . In contrast, the inverse problem provides the learner with a joint distribution  $\pi^*$  and requires finding a cost function  $c^*$  such that  $\pi^*$  becomes the OT plan between its marginals,  $\pi_x^*$  and  $\pi_y^*$ . This setup leads to the formulation of the *inverse entropic OT* problem, which can be expressed as the following minimization problem:

$$c^* \in \arg \min_c \left[ \underbrace{\left( \mathbb{E}_{x, y \sim \pi^*} [c(x, y)] - \varepsilon \mathbb{E}_{x \sim \pi_x^*} \text{H}(\pi^*(\cdot|x)) \right)}_{\geq \text{OT}_{c, \varepsilon}(\pi_x^*, \pi_y^*)} - \text{OT}_{c, \varepsilon}(\pi_x^*, \pi_y^*) \right], \quad (5)$$

where  $c$  skims through measurable functions  $\mathcal{X} \times \mathcal{Y} \rightarrow \mathbb{R}$ . The expression within the parentheses denotes the entropic transport cost of the plan  $\pi^*$  in relation to the cost  $c$  between the marginals  $\pi_x^*$  and  $\pi_y^*$ , thus ensuring that it is always greater than or equal to the optimal cost  $\text{OT}_{c, \varepsilon}(\pi_x^*, \pi_y^*)$ . Consequently, the minimum achievable value for the entire objective is zero, which occurs only when  $\pi^*$  corresponds to the optimal transport plan for the selected cost  $c^*$ . Here, the term  $-\varepsilon \mathbb{E}_{x \sim \pi_x^*} \text{H}(\pi^*(\cdot|x))$  can be omitted, as it does not depend on  $c$ . Additionally

- Unlike the forward OT problem (1), the entropic regularization parameter  $\varepsilon > 0$  here plays no significant role. Indeed, by substituting  $c(x, y) = \frac{\varepsilon}{\varepsilon'} c'(x, y)$  and multiplying the entire objective (5) by  $\frac{\varepsilon'}{\varepsilon}$ , one gets the inverse OT problem for  $\varepsilon'$ . Hence, the problems associated with different  $\varepsilon$  are equivalent up to the change of variables, which is not the case for the forward OT (1).
- The inverse problem admits *several* possible solutions  $c^*$ . For example,  $c^*(x, y) = -\varepsilon \log \pi^*(x, y)$  provides the minimum, which can be verified through direct substitution. Similarly, cost functions of the form  $c^*(x, y) = -\varepsilon \log \pi^*(x, y) + u(x) + v(y)$  are also feasible, as adding terms dependent only on  $x$  or  $y$  does not alter the OT plan. In particular, when  $u(x) = \varepsilon \log \pi_x^*(x)$  and  $v(y) = 0$ , one gets  $c^*(x, y) = -\varepsilon \log \pi^*(y|x)$ .

In practice, the joint distribution  $\pi^*$  is typically available only through empirical samples, meaning that its density is often unknown. As a result, specific solutions such as  $c^*(x, y) = -\varepsilon \log \pi^*(x, y)$  or  $-\varepsilon \log \pi^*(y|x)$  cannot be directly utilized. Consequently, it becomes necessary to develop parametric estimators  $\pi^\theta$  to approximate them using the available samples.

### 3 SEMI-SUPERVISED DOMAIN TRANSLATION VIA INVERSE ENTROPIC OT

In §3.1, we develop our proposed loss function that seamlessly integrates both paired and unpaired data samples. In §3.2, we demonstrate that derived loss is inherently linked to the inverse entropic optimal transport problem (5). In §3.3, we introduce lightweight parametrization to overcome challenges associated with optimizing the loss function. All our proofs can be found in Appendix A.

#### 3.1 LOSS DERIVATION

**Part I. Data likelihood maximization and its limitation.** Our goal is to approximate the true distribution  $\pi^*$  by some parametric model  $\pi^\theta$ , where  $\theta$  represents the parameters of the model. To achieve this, we would like to employ the standard KL-divergence minimization framework, also known as data likelihood maximization. Namely, we aim to minimize

$$\begin{aligned} \text{KL}(\pi^* \parallel \pi^\theta) &= \mathbb{E}_{x, y \sim \pi^*} \log \frac{\pi_x^*(x) \pi^*(y|x)}{\pi_x^\theta(x) \pi^\theta(y|x)} = \mathbb{E}_{x \sim \pi_x^*} \log \frac{\pi_x^*(x)}{\pi_x^\theta(x)} + \mathbb{E}_{x, y \sim \pi^*} \log \frac{\pi^*(y|x)}{\pi^\theta(y|x)} = \\ \text{KL}(\pi_x^* \parallel \pi_x^\theta) &+ \mathbb{E}_{x \sim \pi_x^*} \mathbb{E}_{y \sim \pi^*(\cdot|x)} \log \frac{\pi^*(y|x)}{\pi^\theta(y|x)} = \underbrace{\text{KL}(\pi_x^* \parallel \pi_x^\theta)}_{\text{Marginal}} + \underbrace{\mathbb{E}_{x \sim \pi_x^*} \text{KL}(\pi^*(\cdot|x) \parallel \pi^\theta(\cdot|x))}_{\text{Conditional}}. \end{aligned} \quad (6)$$

It is clear that objective (6) splits into two **independent** components: the *marginal* and the *conditional* matching terms. Our focus will be on the conditional component  $\pi^\theta(\cdot|x)$ , as it is the necessary part for the domain translation. Note that the marginal part  $\pi_x^\theta$  is not actually needed. The conditional part of (6) can further be divided into the following two terms:

$$\mathbb{E}_{x \sim \pi_x^*} \mathbb{E}_{y \sim \pi^*(\cdot|x)} [\log \pi^*(y|x) - \log \pi^\theta(y|x)] = -\mathbb{E}_{x \sim \pi_x^*} \mathbb{H}(\pi^*(\cdot|x)) - \mathbb{E}_{x, y \sim \pi^*} \log \pi^\theta(y|x). \quad (7)$$

The first term is independent on  $\theta$ , so we obtain the following minimization objective

$$\mathcal{L}(\theta) \stackrel{\text{def}}{=} -\mathbb{E}_{x, y \sim \pi^*} \log \pi^\theta(y|x). \quad (8)$$

It is important to note that minimizing (8) is equivalent to maximizing the conditional likelihood, a strategy utilized in conditional normalizing flows (CNFs) (Papamakarios et al., 2021). However, a major limitation of this approach is its reliance solely on paired data from  $\pi^*$ , which can be difficult to obtain in real-world scenarios. In the following section, we modify this strategy to incorporate available unpaired data within a semi-supervised learning setup (see §2.1).

**Part II. Solving the limitations via smart parameterization.** To address the above-mentioned issue and leverage unpaired data, we first use Gibbs-Boltzmann distribution density parametrization:

$$\pi^\theta(y|x) \stackrel{\text{def}}{=} \frac{\exp(-E^\theta(y|x))}{Z^\theta(x)}, \quad (9)$$

where  $E^\theta(\cdot|x) : \mathcal{Y} \rightarrow \mathbb{R}$  is the *Energy function*, and  $Z^\theta(x) \stackrel{\text{def}}{=} \int_{\mathcal{Y}} \exp(-E^\theta(y|x)) dy$  is the normalization constant (LeCun et al., 2006). Substituting (9) into (8), we get

$$-\mathbb{E}_{x, y \sim \pi^*} \log \pi^\theta(y|x) = \mathbb{E}_{x, y \sim \pi^*} E^\theta(y|x) + \mathbb{E}_{x \sim \pi_x^*} \log Z^\theta(x). \quad (10)$$

This objective already provides an opportunity to exploit the unpaired samples from the marginal distribution  $\pi_x^*$  to learn the conditional distributions  $\pi^\theta(\cdot|x) \approx \pi^*(\cdot|x)$ . Namely, it helps to estimate the part of the objective related to the normalization constant  $Z^\theta$ . To incorporate separate samples from the second marginal distribution  $\pi_y^*$ , it is essential to choose a parametrization that allows to detach from the energy function  $E^\theta(y|x)$  the term depending solely on  $y$ . Thus, we propose:

$$E^\theta(y|x) \stackrel{\text{def}}{=} \frac{c^\theta(x, y) - f^\theta(y)}{\varepsilon}. \quad (11)$$

The parameterization in (11) indeed permits the separation of the function  $f^\theta(y)$ . By setting  $f^\theta(y) \equiv 0$  and  $\varepsilon = 0$ , the parameterization of the energy function  $E^\theta(y|x)$  remains consistent, as it can be exclusively derived from  $c^\theta(x, y)$ . Finally, by substituting (11) into (10), we arrive at **our final objective**, which integrates both paired and unpaired data:

$$\mathcal{L}(\theta) = \underbrace{\varepsilon^{-1} \mathbb{E}_{x, y \sim \pi^*} [c^\theta(x, y)]}_{\text{Joint, requires pairs } (x, y) \sim \pi^*} - \underbrace{\varepsilon^{-1} \mathbb{E}_{y \sim \pi_y^*} f^\theta(y)}_{\text{Marginal, requires } x \sim \pi_y^*} - \underbrace{\mathbb{E}_{x \sim \pi_x^*} \log Z^\theta(x)}_{\text{Marginal, requires } x \sim \pi_x^*} \rightarrow \min_{\theta}. \quad (12)$$

At this point, a reader may come up with 2 reasonable questions regarding (12):

1. How to perform the optimization of the proposed objective? This question is not straightforward due to the existence of the (typically intractable) normalizing constant  $Z_\theta$  in the objective.
2. To which extent do the separate terms in (12) (paired, unpaired data) contribute to the objective, and which type of data is the most important for learning the correct solution?

We answer these questions in §3.3 and §5. Before doing that, in the next section, we demonstrate a surprising finding that our proposed objective exactly solves the inverse entropic OT problem (5).

### 3.2 RELATION TO INVERSE ENTROPIC OPTIMAL TRANSPORT

In this section, we show that (5) is equivalent to (12). Indeed, directly substituting the dual form of entropic OT (2) into the inverse entropic OT problem (5) with the omitted entropy term yields:

$$\min_c \left\{ \mathbb{E}_{x, y \sim \pi^*} [c(x, y)] - \max_f \left[ \mathbb{E}_{x \sim \pi_x^*} f^c(x) + \mathbb{E}_{y \sim \pi_y^*} f(y) \right] \right\} = \quad (13)$$

$$\min_{c, f} \left\{ \mathbb{E}_{x, y \sim \pi^*} [c(x, y)] - \mathbb{E}_{x \sim \pi_x^*} f^c(x) - \mathbb{E}_{y \sim \pi_y^*} f(y) \right\}. \quad (14)$$

Now, let's assume that both  $c$  and  $f$  are parameterized as  $c^\theta$  and  $f^\theta$  with respect to a parameter  $\theta$ . Based on the definition provided in (4) and utilizing our energy function parameterization from (11), we can express  $(f^\theta)^{c^\theta}(x)$  as follows:

$$(f^\theta)^{c^\theta}(x) = -\varepsilon \log \int_y \exp \left( \frac{f^\theta(y) - c^\theta(x, y)}{\varepsilon} \right) dy = -\varepsilon \log Z^\theta(x). \quad (15)$$

This clarification shows that the expression in (13) aligns with our proposed likelihood-based loss in (12), scaled by  $\varepsilon$ . This finding indicates that *inverse entropic optimal transport (OT) can be interpreted as a likelihood maximization problem*, which opens up significant avenues to leverage established likelihood maximization techniques for optimizing inverse entropic OT, such as the evidence lower bound methods (Barber, 2012; Alemi et al., 2018) and expectation-maximization strategies (MacKay, 2003; Bishop & Bishop, 2023), etc.

Moreover, this insight allows us to reframe inverse entropic OT as *addressing the semi-supervised domain translation problem*, as it facilitates the use of both paired data from  $\pi^*$  and unpaired data from  $\pi_x^*$  and  $\pi_y^*$ . Notably, to our knowledge, the inverse OT problem has primarily been explored in *discrete* learning scenarios that assume access only to paired data (refer to §4).

### 3.3 PRACTICAL LIGHT PARAMETERIZATION AND OPTIMIZATION PROCEDURE

The most computationally intensive aspect of optimizing the loss function in (12) lies in calculating the integral for the normalization constant  $Z^\theta$ . To tackle this challenge, we propose a lightweight parameterization that yields closed-form expressions for each term in the loss function. Our proposed cost function parameterization  $c^\theta$  is grounded in the LOG-SUM-EXP function (Murphy, 2012), which is widely recognized in the deep learning community for its practical advantages:

$$c^\theta(x, y) = -\varepsilon \log \sum_{m=1}^M v_m^\theta(x) \exp \left( \frac{\langle b_m^\theta(x), y \rangle}{\varepsilon} \right), \quad (16)$$

where  $\{w_m^\theta(x) : \mathbb{R}^{D_x} \rightarrow \mathbb{R}_+, b_m^\theta(x) : \mathbb{R}^{D_x} \rightarrow \mathbb{R}^{D_y}\}_{m=1}^M$  are arbitrary parametric functions, e.g., *neural networks*, with learnable parameters denoted by  $\theta_c$ . Inspired by the work (Korotin et al., 2024), we employ Gaussian mixture parametrization in the dual potential  $f^\theta$ :

$$f^\theta(y) = \varepsilon \log \sum_{n=1}^N w_n^\theta \mathcal{N}(y | a_n^\theta, \varepsilon A_n^\theta), \quad (17)$$

where  $\theta_f \stackrel{\text{def}}{=} \{w_n^\theta, a_n^\theta, A_n^\theta\}_{n=1}^N$  are learnable parameters of the potential, with  $w_n^\theta \geq 0$ ,  $a_n^\theta \in \mathbb{R}^{D_y}$ , and  $A_n^\theta \in \mathbb{R}^{D_y \times D_y}$  being a symmetric positive definite matrix. Thereby, our framework comprises a total of  $\theta \stackrel{\text{def}}{=} \theta_f \cup \theta_c$  learnable parameters. For *clarity* and to *avoid notation overload*, we will omit the superscript  $^\theta$  associated learnable parameters and functions in the subsequent formulas.

**Proposition 3.1** (Tractable form of the normalization constant). *Our parametrization of the cost function (16) and dual potential (17) delivers  $Z^\theta(x) \stackrel{\text{def}}{=} \sum_{m=1}^M \sum_{n=1}^N z_{mn}(x)$ , where*

$$z_{mn}(x) \stackrel{\text{def}}{=} w_n v_m(x) \exp\left(\frac{b_m^\top(x) A_n b_m(x) + 2a_n^\top b_m(x)}{2\varepsilon}\right). \quad (18)$$

The proposition offers a closed-form expression for  $Z^\theta(x)$ , which is essential for optimizing (12). Furthermore, the following proposition provides a method for sampling  $y$  given a new sample  $x_{\text{new}}$ .

**Proposition 3.2** (Tractable form of the conditional distributions). *From our parametrization of the cost function (16) and dual potential (17) it follows that the  $\pi^\theta(\cdot|x)$  are Gaussian mixtures:*

$$\pi^\theta(y|x) = \frac{1}{Z^\theta(x)} \sum_{m=1}^M \sum_{n=1}^N z_{mn}(x) \mathcal{N}(y | s_{mn}(x), \varepsilon A_n), \quad (19)$$

where  $s_{mn}(x) \stackrel{\text{def}}{=} a_n + A_n b_m(x)$  and  $z_{mn}(x)$  defined in Proposition 3.1.

TRAINING. As stated in §2.1, since we only have access to the samples from the distributions, we will optimize the empirical counterpart of (12) via stochastic gradient descent in the parameters  $\theta$ :

$$\mathcal{L}(\theta) \approx \widehat{\mathcal{L}}(\theta) \stackrel{\text{def}}{=} \frac{1}{P} \sum_{p=1}^P c^\theta(x_p, y_p) - \frac{1}{Q} \sum_{q=1}^Q [-\varepsilon \log Z^\theta(x_q)] - \frac{1}{R} \sum_{r=1}^R f^\theta(y_r) \rightarrow \min_{\theta}. \quad (20)$$

INFERENCE. According to our Proposition 3.2, the conditional distributions  $\pi^\theta(\cdot|x)$  are Gaussian mixtures (19). As a result, sampling  $y$  given  $x$  is straightforward and light-speed.

## 4 RELATED WORKS

We review below the most related semi-supervised models and OT-based approaches to our work.

**Semi-supervised models.** As mentioned in §1, many existing semi-supervised domain translation methods combine paired and unpaired data by incorporating multiple loss terms into complex optimization objectives (Jin et al., 2019, §3.3), (Tripathy et al., 2019, §3.5), (Mustafa & Mantiuk, 2020, §3.2), (Paavilainen et al., 2021, §2), (Panda et al., 2023, Eq. 8), (Tang et al., 2024, Eq. 8). However, these approaches often require careful tuning of hyperparameters to balance the various loss terms.

The recent work by (Gu et al., 2023) utilizes both paired and unpaired data to build a transport plan based on key-point guided OT, initially introduced in (Gu et al., 2022). This transport plan is used as a heuristic to train a conditional score-based model on unpaired or semi-paired data. Overall, we note that the idea of applying OT in a semi-supervised manner traces back to the seminal work by (Courty et al., 2016), although their focus was on classification, not domain translation.

Another recent work by (Asadulaev et al., 2024) introduces a neural network-based OT framework for semi-supervised scenarios, utilizing general cost functionals for OT. However, their method requires **manually** constructing cost functions which can incorporate class labels or predefined pairs. In contrast, our approach adjusts the cost dynamically during training.

**(Inverse) OT solvers.** Our approach builds upon the light OT methods proposed by (Korotin et al., 2024; Gushchin et al., 2024), which introduce a *forward* solver for the entropic OT problem with the quadratic cost function  $c^*(x, y) = \frac{1}{2}\|x - y\|_2^2$  using the Gaussian Mixture parametrization. However, we consider a more general cost function (16) and incorporate cost function learning directly into the objective (20), in fact, producing an *inverse* OT (5) solver.

As highlighted in §2.2, the task of inverse optimal transport (IOT) implies learning the cost function from samples drawn from an optimal coupling  $\pi^*$ . Existing IOT solvers (Dupuy & Galichon, 2014; Dupuy et al., 2016; Li et al., 2019; Stuart & Wolfram, 2020; Ma et al., 2020; Chiu et al., 2022; Galichon & Salanié, 2022) focus on reconstructing cost functions from discrete marginal distributions, in particular, using the log-likelihood maximization techniques (Dupuy et al., 2016), see the introduction of (Andrade et al., 2023) for a review. In contrast, we develop a log-likelihood based approach aimed at learning a conditional distribution  $\pi^\theta(\cdot|x) \approx \pi^*(\cdot|x)$  that incorporates both paired and unpaired data but not the cost function itself.

Recent work by (Howard et al., 2024) proposes a framework for learning cost functions to improve the mapping between the domains. However, it is limited by the use of deterministic mappings, i.e., does not have the ability to model non-degenerate conditional distributions.

## 5 EXPERIMENTAL ILLUSTRATIONS

We tested our solver on both synthetic data (§5.1) and real-world data distributions (§5.2). The code is written using the PyTorch framework and will be made publicly available. It is provided in the supplemental materials. Experimental details are given in Appendix B.

### 5.1 SWISS ROLL

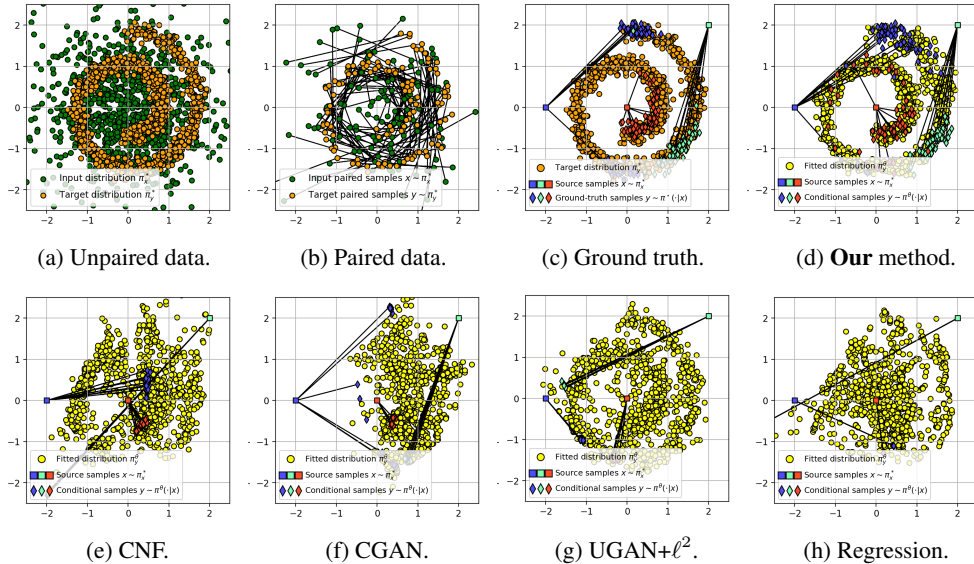


Figure 2: Comparison of the learned mapping on *Gaussian*  $\rightarrow$  *Swiss Roll* task. We use  $P = 128$  paired data,  $Q = 1024$  and  $R = 1024$  unpaired source and target data, respectively.

**Setup.** For illustration purposes, we adapt the setup described in (Mokrov et al., 2024; Korotin et al., 2024) for our needs and consider a synthetic task where we transform samples from a Gaussian distribution  $\pi_x^*$  into a Swiss Roll  $\pi_y^*$  distribution (Figure 2a). The plan  $\pi^*$  is generated by sampling from the mini-batch OT plan using the POT library (Flamary et al., 2021). We specifically chose a transportation cost for the minibatch OT to construct an optimal plan  $\pi^*$  with bi-modal conditional distributions  $\pi^*(\cdot|x)$  to assess how well our method performs in such a scenario. See Appendix B.2.1 for more details. During training, we use  $P = 128$  paired (Figure 2b) and  $Q = R = 1024$



unpaired samples. For an ablation study on how varying amounts of paired and unpaired data affect our method’s performance, see Appendix B.2.4.

**Baselines.** We compare our method against several well-known generative modeling techniques, including: Conditional Normalizing Flow (Winkler et al., 2019, CNF), Conditional Generative Adversarial Network (Mirza & Osindero, 2014, CGAN), Unconditional GAN (Goodfellow et al., 2014) with  $\ell^2$  loss supplement (UGAN+ $\ell^2$ ), and just multilayer perceptron (MLP) regression with  $\ell^2$  loss. For a detailed explanation of baselines employed in our experiments, please see Appendix B.2.2. Some of the baseline methods can fully utilize both paired and unpaired data during training, while others can use paired data only, see Table 1. **Discussion.** The results of the aforementioned meth-

Method	Paired $(x, y) \sim \pi^*$	Unpaired $x \sim \pi_x^*$	Unpaired $y \sim \pi_y^*$
<i>Conditional NF</i>	✓	✗	✗
<i>Conditional GAN</i>	✓	✓	✗
<i>Unconditional GAN + <math>\ell^2</math></i>	✓	✓	✓
<i>Regression</i>	✓	✗	✗
<b><i>Our method</i></b>	✓	✓	✓

Table 1: The ability to use of paired/unpaired data by various models.

ods are depicted in Figure 2. Clearly, the Regression model simply predicts the conditional mean  $\mathbb{E}_{y \sim \pi^*(\cdot|x)} y$ , failing to capture the full distribution. The CNF model suffers from overfitting, likely due to the limited availability of paired data  $XY_{\text{paired}}$ . The CGAN is unable to accurately learn the target distribution  $\pi_y^*$ , while the UGAN+ $\ell^2$  fails to capture the underlying conditional distribution, resulting in suboptimal performance. As a sanity check, we evaluate all baselines using a large amount of paired data. Details are given in Appendix B.2.3.

## 5.2 WEATHER PREDICTION

Here we aim to evaluate our proposed approach on real-world data. We consider the *weather prediction* dataset (Malinin et al., 2021; Rubachev et al., 2024). The data is collected from weather stations and weather forecast physical models. It consists of 94 meteorological features, e.g., pressure, wind, humidity, etc., which are measured over a period of one year at different spatial locations.

**Setup.** Initially, the problem was formulated as the prediction and uncertainty estimation of the air temperature at a specific time and location. We expand this task to the probabilistic prediction of all meteorological features, thereby reducing reliance on measurement equipment in remote and difficult-to-access locations, such as the Polar regions.

In more detail, we select two distinct months from the dataset and translate the meteorological features from the source month (January) to the target month (June). To operate at the monthly scale, we represent a source data point  $x \in \mathbb{R}^{188}$  as the mean and standard deviation of the features collected at a specific location over the source month. The targets  $y \in \mathbb{R}^{94}$  correspond to individual measurements in the target month. Pairs are constructed by aligning a source data point with the target measurements at the same location. Consequently, multiple target data points  $y$  may correspond to a single source point  $x$  and represent samples from conditional distributions  $\pi^*(y|x)$ . The measurements from non-aligned locations are treated as unpaired.

We obtain 500 unpaired and 192 paired data samples. For testing, 100 pairs are randomly selected. We evaluate the performance of our approach by calculating the *log-likelihood* on the test target features. A natural baseline for this task is a probabilistic model that maximizes the likelihood of the target data. Thus, we implement an MLP that learns to predict the parameters of a mixture of Gaussians and is trained on the paired data only via the log-likelihood optimization (8).

**Results.** The results are presented in Table 2. Our experiments demonstrate that increasing the number of paired and unpaired data samples leads to improved test *log-likelihood*, which highlights the impact of the objective that employs both paired and unpaired data. Moreover, the proposed approach outperforms the baseline solution, which shows that even in problems where the paired data plays a key role for accurate predictions, incorporating the unpaired data can give an advantage.

		Baseline			Ours		
#paired \ #unpaired		0	10	50	100	250	500
	10	$0.4 \pm .2$	$17.9 \pm .3$	$18.5 \pm .4$	$18.4 \pm .2$	$18.8 \pm .2$	$19.2 \pm .3$
	25	$3.5 \pm .09$	$18.3 \pm .06$	$18.7 \pm .2$	$18.8 \pm .07$	$19.5 \pm .1$	$19.8 \pm .1$
	50	$6.4 \pm .05$	$18.7 \pm .2$	$18.9 \pm .04$	$19.2 \pm .2$	$19.8 \pm .03$	$20.3 \pm .4$
	90	$6.5 \pm .1$	$19 \pm .01$	$19.4 \pm .05$	$19.4 \pm .2$	$20.3 \pm .05$	$20.5 \pm .09$

Table 2: The values of the test *log-likelihood*  $\uparrow$  on the *weather prediction* dataset obtained for a different number of paired and unpaired training samples.

## 6 DISCUSSION

**Limitations.** A limitation of our approach is that it uses the Gaussian Mixture parameterization for conditional distributions. This may limit its scalability. As a promising avenue for future work is incorporation of the more general parameterizations, such as neural networks, which are already well-studied in the context of forward entropic OT, see (Mokrov et al., 2024).

**Potential impact.** Our framework has a simple and non-minimax optimization objective that seamlessly incorporates both unpaired and paired samples into the training. We expect that these advantages will encourage the use of our framework to develop other max-likelihood-based semi-supervised approaches based on more advanced (than Gaussian mixtures) techniques, e.g., energy-based models (LeCun et al., 2006; Du & Mordatch, 2019), diffusion models (Ho et al., 2020), etc.

**Broader impact.** This paper presents work whose goal is to advance the field of Machine Learning. There are many potential societal consequences of our work, none of which we feel must be specifically highlighted here.

**Reproducibility Statement** For all the presented experiments, a full set of hyperparameters is introduced either in §5 or in Appendix B. In addition, the code is submitted as supplementary material, with guidelines on how to run every experiment included.

## ACKNOWLEDGMENTS

Skoltech was supported by the Analytical center under the RF Government (subsidy agreement 000000D730321P5Q0002, Grant No. 70-2021-00145 02.11.2021).

## REFERENCES

- Abien Fred Agarap. Deep learning using rectified linear units (relu). *arXiv preprint arXiv:1803.08375*, 2018.
- Alexander Alemi, Ben Poole, Ian Fischer, Joshua Dillon, Rif A Saurous, and Kevin Murphy. Fixing a broken elbow. In *International conference on machine learning*, pp. 159–168. PMLR, 2018.
- Francisco Andrade, Gabriel Peyré, and Clarice Poon. Sparsistency for inverse optimal transport. *arXiv preprint arXiv:2310.05461*, 2023.
- Jason Ansel, Edward Yang, Horace He, Natalia Gimelshein, Animesh Jain, Michael Voznesensky, Bin Bao, Peter Bell, David Berard, Evgeni Burovski, Geeta Chauhan, Anjali Chourdia, Will Constable, Alban Desmaison, Zachary DeVito, Elias Ellison, Will Feng, Jiong Gong, Michael Gschwind, Brian Hirsh, Sherlock Huang, Kshiteej Kalambarakar, Laurent Kirsch, Michael Lazos, Mario Lezcano, Yanbo Liang, Jason Liang, Yinghai Lu, CK Luk, Bert Maher, Yunjie Pan, Christian Puhersch, Matthias Reso, Mark Saroufim, Marcos Yukio Siraichi, Helen Suk, Michael Suo, Phil Tillet, Eikan Wang, Xiaodong Wang, William Wen, Shunting Zhang, Xu Zhao, Keren Zhou, Richard Zou, Ajit Mathews, Gregory Chanan, Peng Wu, and Soumith Chintala. Pytorch 2: Faster machine learning through dynamic python bytecode transformation and graph compilation. In *29th ACM International Conference on Architectural Support for Programming Languages and*

- Operating Systems, Volume 2 (ASPLOS '24)*. ACM, April 2024. doi: 10.1145/3620665.3640366. URL <https://pytorch.org/assets/pytorch2-2.pdf>.
- Arip Asadulaev, Alexander Korotin, Vage Egiazarian, Petr Mokrov, and Evgeny Burnaev. Neural optimal transport with general cost functionals. In *The Twelfth International Conference on Learning Representations*, 2024.
- Andrei Atanov, Alexandra Volokhova, Arsenii Ashukha, Ivan Sosnovik, and Dmitry Vetrov. Semi-conditional normalizing flows for semi-supervised learning. *arXiv preprint arXiv:1905.00505*, 2019.
- Julio Backhoff-Veraguas and Gudmund Pammer. Applications of weak transport theory. *Bernoulli*, 28(1):370–394, 2022.
- Julio Backhoff-Veraguas, Mathias Beiglböck, and Gudmun Pammer. Existence, duality, and cyclical monotonicity for weak transport costs. *Calculus of Variations and Partial Differential Equations*, 58(6):203, 2019.
- David Barber. *Bayesian reasoning and machine learning*. Cambridge University Press, 2012.
- Christopher M Bishop and Hugh Bishop. *Deep learning: Foundations and concepts*. Springer Nature, 2023.
- Wei-Ting Chiu, Pei Wang, and Patrick Shafto. Discrete probabilistic inverse optimal transport. In *International Conference on Machine Learning*, pp. 3925–3946. PMLR, 2022.
- Nicolas Courty, Rémi Flamary, Devis Tuia, and Alain Rakotomamonjy. Optimal transport for domain adaptation. *IEEE transactions on pattern analysis and machine intelligence*, 39(9):1853–1865, 2016.
- Marco Cuturi. Sinkhorn distances: Lightspeed computation of optimal transport. *Advances in neural information processing systems*, 26, 2013.
- Laurent Dinh, Jascha Sohl-Dickstein, and Samy Bengio. Density estimation using real NVP. In *International Conference on Learning Representations*, 2017. URL <https://openreview.net/forum?id=HkpbhH9lx>.
- Yichao Du, Weizhi Wang, Zhirui Zhang, Boxing Chen, Tong Xu, Jun Xie, and Enhong Chen. Non-parametric domain adaptation for end-to-end speech translation. In *Conference on Empirical Methods in Natural Language Processing (EMNLP)*, 2022.
- Yilun Du and Igor Mordatch. Implicit generation and modeling with energy based models. *Advances in Neural Information Processing Systems*, 32, 2019.
- Arnaud Dupuy and Alfred Galichon. Personality traits and the marriage market. *Journal of Political Economy*, 122(6):1271–1319, 2014.
- Arnaud Dupuy, Alfred Galichon, and Yifei Sun. Estimating matching affinity matrix under low-rank constraints. *arXiv preprint arXiv:1612.09585*, 2016.
- Rémi Flamary, Nicolas Courty, Alexandre Gramfort, Mokhtar Z Alaya, Aurélie Boisbunon, Stanislas Chambon, Laetitia Chapel, Adrien Corenflos, Kilian Fatras, Nemo Fournier, et al. Pot: Python optimal transport. *Journal of Machine Learning Research*, 22(78):1–8, 2021.
- Alfred Galichon and Bernard Salanié. Cupid’s invisible hand: Social surplus and identification in matching models. *The Review of Economic Studies*, 89(5):2600–2629, 2022.
- Aude Genevay. *Entropy-regularized optimal transport for machine learning*. PhD thesis, Université Paris sciences et lettres, 2019.
- Ian Goodfellow, Jean Pouget-Abadie, Mehdi Mirza, Bing Xu, David Warde-Farley, Sherjil Ozair, Aaron Courville, and Yoshua Bengio. Generative adversarial nets. *Advances in neural information processing systems*, 27, 2014.

- Nathael Gozlan, Cyril Roberto, Paul-Marie Samson, and Prasad Tetali. Kantorovich duality for general transport costs and applications. *Journal of Functional Analysis*, 273(11):3327–3405, 2017.
- Xiang Gu, Yucheng Yang, Wei Zeng, Jian Sun, and Zongben Xu. Keypoint-guided optimal transport with applications in heterogeneous domain adaptation. *Advances in Neural Information Processing Systems*, 35:14972–14985, 2022.
- Xiang Gu, Liwei Yang, Jian Sun, and Zongben Xu. Optimal transport-guided conditional score-based diffusion model. *Advances in Neural Information Processing Systems*, 36:36540–36552, 2023.
- Nikita Gushchin, Alexander Kolesov, Petr Mokrov, Polina Karpikova, Andrei Spiridonov, Evgeny Burnaev, and Alexander Korotin. Building the bridge of schrödinger: A continuous entropic optimal transport benchmark. *Advances in Neural Information Processing Systems*, 36:18932–18963, 2023.
- Nikita Gushchin, Sergei Kholkin, Evgeny Burnaev, and Alexander Korotin. Light and optimal schrödinger bridge matching. In *Forty-first International Conference on Machine Learning*, 2024.
- Simon Haykin. *Neural networks: a comprehensive foundation*. Prentice Hall PTR, 1998.
- Jonathan Ho, Ajay Jain, and Pieter Abbeel. Denoising diffusion probabilistic models. *Advances in neural information processing systems*, 33:6840–6851, 2020.
- Samuel Howard, George Deligiannidis, Patrick Rebeschini, and James Thornton. Differentiable cost-parameterized monge map estimators. *arXiv preprint arXiv:2406.08399*, 2024.
- Pavel Izmailov, Polina Kirichenko, Marc Finzi, and Andrew Gordon Wilson. Semi-supervised learning with normalizing flows. In *International conference on machine learning*, pp. 4615–4630. PMLR, 2020.
- Qingnan Jiang, Mingxuan Wang, Jun Cao, Shanbo Cheng, Shujian Huang, and Lei Li. Learning kernel-smoothed machine translation with retrieved examples. In *Conference on Empirical Methods in Natural Language Processing (EMNLP)*, 2021.
- Yuxin Jiang, Liming Jiang, Shuai Yang, and Chen Change Loy. Scenimefy: Learning to craft anime scene via semi-supervised image-to-image translation. In *IEEE International Conference on Computer Vision (ICCV)*, 2023.
- Cheng-Bin Jin, Hakil Kim, Mingjie Liu, Wonmo Jung, Seongsu Joo, Eunsik Park, Young Saem Ahn, In Ho Han, Jae Il Lee, and Xuenan Cui. Deep ct to mr synthesis using paired and unpaired data. *Sensors*, 19(10):2361, 2019.
- Leonid V Kantorovich. On the translocation of masses. In *Dokl. Akad. Nauk. USSR (NS)*, volume 37, pp. 199–201, 1942.
- Diederik P Kingma. Adam: A method for stochastic optimization. *arXiv preprint arXiv:1412.6980*, 2014.
- Alexander Korotin, Nikita Gushchin, and Evgeny Burnaev. Light schrödinger bridge. In *The Twelfth International Conference on Learning Representations*, 2024.
- Yann LeCun, Sumit Chopra, Raia Hadsell, M Ranzato, Fugie Huang, et al. A tutorial on energy-based learning. *Predicting structured data*, 1(0), 2006.
- Ruilin Li, Xiaojing Ye, Haomin Zhou, and Hongyuan Zha. Learning to match via inverse optimal transport. *Journal of machine learning research*, 20(80):1–37, 2019.
- Jianxin Lin, Yingce Xia, Tao Qin, Zhibo Chen, and Tie-Yan Liu. Conditional image-to-image translation. In *Computer Vision and Pattern Recognition (CVPR)*, 2018.
- Shaojun Ma, Haodong Sun, Xiaojing Ye, Hongyuan Zha, and Haomin Zhou. Learning cost functions for optimal transport. *arXiv preprint arXiv:2002.09650*, 2020.

- David JC MacKay. *Information theory, inference and learning algorithms*. Cambridge university press, 2003.
- Andrey Malinin, Neil Band, German Chesnokov, Yarin Gal, Mark JF Gales, Alexey Noskov, Andrey Ploskonosov, Liudmila Prokhorenkova, Ivan Provilkov, Vatsal Raina, et al. Shifts: A dataset of real distributional shift across multiple large-scale tasks. *arXiv preprint arXiv:2107.07455*, 2021.
- Mehdi Mirza and Simon Osindero. Conditional generative adversarial nets. *CoRR*, abs/1411.1784, 2014. URL <http://arxiv.org/abs/1411.1784>.
- Petr Mokrov, Alexander Korotin, Alexander Kolesov, Nikita Gushchin, and Evgeny Burnaev. Energy-guided entropic neural optimal transport. In *The Twelfth International Conference on Learning Representations*, 2024.
- Nikita Moriakov, Jonas Adler, and Jonas Teuwen. Kernel of cyclegan as a principal homogeneous space. In *International Conference on Learning Representations*, 2020.
- Makoto Morishita, Jun Suzuki, and Masaaki Nagata. Domain adaptation of machine translation with crowdworkers. In *Conference on Empirical Methods in Natural Language Processing (EMNLP)*, 2022.
- Kevin P Murphy. *Machine learning: a probabilistic perspective*. MIT press, 2012.
- Aamir Mustafa and Rafał K Mantiuk. Transformation consistency regularization—a semi-supervised paradigm for image-to-image translation. In *Computer Vision—ECCV 2020: 16th European Conference, Glasgow, UK, August 23–28, 2020, Proceedings, Part XVIII 16*, pp. 599–615. Springer, 2020.
- Pauliina Paavilainen, Saad Ullah Akram, and Juho Kannala. Bridging the gap between paired and unpaired medical image translation. In *MICCAI Workshop on Deep Generative Models*, pp. 35–44. Springer, 2021.
- Nishant Panda, Natalie Klein, Dominic Yang, Patrick Gasda, and Diane Oyen. Semi-supervised learning of pushforwards for domain translation & adaptation. *arXiv preprint arXiv:2304.08673*, 2023.
- George Papamakarios, Eric Nalisnick, Danilo Jimenez Rezende, Shakir Mohamed, and Balaji Lakshminarayanan. Normalizing flows for probabilistic modeling and inference. *Journal of Machine Learning Research*, 22(57):1–64, 2021.
- Duo Peng, Ping Hu, Qihong Ke, and Jun Liu. Diffusion-based image translation with label guidance for domain adaptive semantic segmentation. In *IEEE International Conference on Computer Vision (ICCV)*, 2023.
- Gabriel Peyré, Marco Cuturi, et al. Computational optimal transport: With applications to data science. *Foundations and Trends® in Machine Learning*, 11(5-6):355–607, 2019.
- Ivan Rubachev, Nikolay Kartashev, Yury Gorishniy, and Artem Babenko. Tabred: A benchmark of tabular machine learning in-the-wild. *arXiv preprint arXiv:2406.19380*, 2024.
- Filippo Santambrogio. Optimal transport for applied mathematicians. *Birkäuser, NY*, 55(58-63):94, 2015.
- Andrew M Stuart and Marie-Therese Wolfram. Inverse optimal transport. *SIAM Journal on Applied Mathematics*, 80(1):599–619, 2020.
- Xiaole Tang, Xin Hu, Xiang Gu, and Jian Sun. Residual-conditioned optimal transport: Towards structure-preserving unpaired and paired image restoration. In *Forty-first International Conference on Machine Learning*, 2024. URL <https://openreview.net/forum?id=irBHP1knxP>.
- Soumya Tripathy, Juho Kannala, and Esa Rahtu. Learning image-to-image translation using paired and unpaired training samples. In *Computer Vision—ACCV 2018: 14th Asian Conference on Computer Vision, Perth, Australia, December 2–6, 2018, Revised Selected Papers, Part II 14*, pp. 51–66. Springer, 2019.

Florin-Alexandru Vasluianu, Andrés Romero, Luc Van Gool, and Radu Timofte. Shadow removal with paired and unpaired learning. In *Proceedings of the IEEE/CVF Conference on Computer Vision and Pattern Recognition*, pp. 826–835, 2021.

Cédric Villani et al. *Optimal transport: old and new*, volume 338. Springer, 2009.

Christina Winkler, Daniel E. Worrall, Emiel Hoogeboom, and Max Welling. Learning likelihoods with conditional normalizing flows. *CoRR*, abs/1912.00042, 2019. URL <http://arxiv.org/abs/1912.00042>.

Xiaohe Wu, Ming Liu, Yue Cao, Dongwei Ren, and Wangmeng Zuo. Unpaired learning of deep image denoising. In *European conference on computer vision*, pp. 352–368. Springer, 2020.

Zaifeng Yang and Zhenghua Chen. Learning from paired and unpaired data: Alternately trained cyclegan for near infrared image colorization. In *2020 IEEE International Conference on Visual Communications and Image Processing (VCIP)*, pp. 467–470. IEEE, 2020.

Yuan Yuan, Siyuan Liu, Jiawei Zhang, Yongbing Zhang, Chao Dong, and Liang Lin. Unsupervised image super-resolution using cycle-in-cycle generative adversarial networks. In *Proceedings of the IEEE conference on computer vision and pattern recognition workshops*, pp. 701–710, 2018.

Jun-Yan Zhu, Taesung Park, Phillip Isola, and Alexei A Efros. Unpaired image-to-image translation using cycle-consistent adversarial networks. In *Proceedings of the IEEE international conference on computer vision*, pp. 2223–2232, 2017.

## A PROOFS

*Proof of Proposition 3.1.* Thanks to our parametrization of the cost  $c^\theta$  (16) and the dual potential  $f^\theta$  (17), we obtain:

$$\begin{aligned} \exp\left(\frac{f^\theta(y) - c^\theta(x, y)}{\varepsilon}\right) &= \exp\left(\log \sum_{n=1}^N w_n \mathcal{N}(y | a_n, \varepsilon A_n) + \log \sum_{m=1}^M v_m(x) \exp\left(\frac{\langle b_m(x), y \rangle}{\varepsilon}\right)\right) \\ &= \sum_{m=1}^M \sum_{n=1}^N \frac{v_m(x) w_n}{\sqrt{\det(2\pi A_n^{-1})}} \exp\left(-\frac{1}{2}(y - a_n)^\top \frac{A_n^{-1}}{\varepsilon} (y - a_n) + \frac{\langle b_m(x), y \rangle}{\varepsilon}\right) \end{aligned}$$

Now we need to transform the expression above into the form of a Gaussian Mixture Model. To achieve this, we rewrite the formula inside the exponent using the fact that  $A_n$  is a symmetric:

$$\begin{aligned} (y - a_n)^\top A_n^{-1} (y - a_n) - 2\langle b_m(x), y \rangle &= y^\top A_n^{-1} y - 2a_n^\top A_n^{-1} y + a_n^\top A_n^{-1} a_n - 2\langle b_m(x), y \rangle = \\ &= y^\top A_n^{-1} y - 2 \underbrace{(a_n + A_n b_m(x))^\top}_{\stackrel{\text{def}}{=} s_{mn}^\top(x)} A_n^{-1} y + a_n^\top A_n^{-1} a_n = \\ &= (y - s_{mn}(x))^\top A_n^{-1} (y - s_{mn}(x)) + a_n^\top A_n^{-1} a_n - s_{mn}^\top(x) A_n^{-1} s_{mn}(x). \end{aligned}$$

Afterwards, we rewrite the last two terms:

$$\begin{aligned} a_n^\top A_n^{-1} a_n - s_{mn}^\top(x) A_n^{-1} s_{mn}(x) &= a_n^\top A_n^{-1} a_n - (a_n + A_n b_m(x))^\top A_n^{-1} (a_n + A_n b_m(x)) = \\ a_n^\top A_n^{-1} a_n - a_n^\top A_n^{-1} a_n - a_n^\top A_n^{-1} A_n b_m(x) - b_m^\top(x) A_n A_n^{-1} a_n - b_m^\top(x) A_n A_n^{-1} A_n b_m(x) &= \\ -b_m^\top(x) A_n b_m(x) - 2a_n^\top b_m(x). \end{aligned}$$

Finally, we get

$$\begin{aligned} \exp\left(\frac{f^\theta(y) - c^\theta(x, y)}{\varepsilon}\right) &= \sum_{m=1}^M \sum_{n=1}^N \underbrace{w_n v_m(x) \exp\left(\frac{b_m^\top(x) A_n b_m(x) + 2a_n^\top b_m(x)}{2\varepsilon}\right)}_{\stackrel{\text{def}}{=} z_{mn}(x)} \\ &\cdot \underbrace{\frac{1}{\sqrt{\det(2\pi A_n^{-1})}} \exp\left(-\frac{1}{2}(y - s_{mn}(x))^\top \frac{A_n^{-1}}{\varepsilon} (y - s_{mn}(x))\right)}_{= \mathcal{N}(y | s_{mn}(x), \varepsilon A_n)}, \end{aligned}$$

and thanks to  $\int_{\mathcal{Y}} \mathcal{N}(y | s_{mn}(x), \varepsilon A_n) dy = 1$ , the normalization constant simplifies to the sum of  $z_{mn}(x)$ :

$$\begin{aligned} Z^\theta(x) &= \int_{\mathcal{Y}} \exp\left(\frac{f^\theta(y) - c^\theta(x, y)}{\varepsilon}\right) dy \\ &= \int_{\mathcal{Y}} \sum_{m=1}^M \sum_{n=1}^N z_{mn}(x) \mathcal{N}(y | s_{mn}(x), \varepsilon A_n) dy = \sum_{m=1}^M \sum_{n=1}^N z_{mn}(x). \end{aligned}$$

□

*Proof of Proposition 3.2.* Combining equations (9), (11) and derivation above, we seamlessly obtain the expression (19) needed for Proposition 3.2. □

## B DETAILS OF THE EXPERIMENTS

### B.1 GENERAL IMPLEMENTATION DETAILS

To minimize (20), we parameterize  $f^\theta$  (17) by representing  $w_n$  using  $\log w_n, a_n$  directly as a vector, and the matrix  $A_n$  in diagonal form with  $\log(A_n)_{i,i}$  on its diagonal. For  $c^\theta$  (16), we parameterize  $v_m(x)$  as a multilayer perceptron (MLP) (Haykin, 1998) with ReLU activations (Agarap, 2018) and a LogSoftMax output layer, while  $b_m(x)$  is also modeled as an MLP with ReLU activations. The depth and number of hidden layers vary depending on the experiment.

To further simplify optimization, we use diagonal matrices  $A_n$  in the parameterization of  $f^\theta$ , which not only significantly reduces the number of learnable parameters in  $\theta_f$ , but also enables efficient computation of  $A_n^{-1}$  with a time complexity of  $\mathcal{O}(D_y)$ .

We utilize two separate Adam optimizers (Kingma, 2014) with different step sizes for paired and unpaired data to improve convergence.

As mentioned in §2.2, the solver is independent of  $\varepsilon$ , so we set  $\varepsilon = 1$  for all experiments.

**Initialization.** We initialize  $\log w_n$  as  $\log \frac{1}{n}$ , set  $a_n$  using random samples from  $\pi_y^*$ , and initialize  $\log(A_n)_{i,i}$  with  $\log(0.1)$ . For the neural networks, we apply the default PyTorch (Ansel et al., 2024) initialization.

### B.2 GAUSSIAN TO SWISS ROLL MAPPING

In all experiments conducted in this section, we set the parameters as follows:  $N = 50, M = 25$ , with learning rates  $lr_{\text{paired}} = 3 \times 10^{-4}$  and  $lr_{\text{unpaired}} = 0.001$ . We utilize a two-layer MLP network for the function  $b_m(x)$  and a single-layer MLP for  $v_m(x)$ . The experiments are executed in parallel on a 2080 Ti GPU for a total of 25,000 iterations, taking approximately 20 minutes to complete.

#### B.2.1 TRANSPORTATION COST MATRIX

To create the ground truth plan  $\pi^*$ , we utilize the following procedure: We start by sampling a mini-batch of size 64 and then determine the optimal mapping using the entropic Sinkhorn algorithm, as outlined in (Cuturi, 2013) and implemented in (Flamary et al., 2021). This process is repeated  $P$  times to generate the required number of pairs.

We define the cost matrix for mini-batch OT as  $C = \min(C^\varphi, C^{-\varphi})$ , where  $C^{\pm\varphi}$  represents matrices of pairwise  $\ell_2$  distances between  $x$  and  $-y^{\pm\varphi}$ , with  $-y^{\pm\varphi}$  denoting the vector  $-y$  rotated by an angle of  $\varphi = \pm 90^\circ$ . In other words,  $x \sim \pi_x^*$  maps to  $y$  located on the opposite side of the Swiss Roll, rotated by either  $\varphi$  or  $-\varphi$ , as shown in Figure 2c.

#### B.2.2 DISCUSSION OF THE BASELINES

In this section, we discuss the losses used by the baseline models in order to explain Table 1.

- **Regression Model** (MLP) uses the following simple  $\ell^2$  loss

$$\min_{\psi} \mathbb{E}_{(x,y) \sim \pi^*} \|y - G_{\theta}(x)\|^2,$$

where  $G_{\theta} : \mathcal{X} \rightarrow \mathcal{Y}$  is a generator MLP with trainable parameters  $\theta$ . Clearly, such a model can use only paired data. Furthermore, it is known that the optimal regressor  $G^*$  coincides with  $\mathbb{E}_{y \sim \pi^*(\cdot|x)} y$ , i.e., predicts the conditional expectation. Therefore, such a model will never learn the true data distribution unless all  $\pi^*(\cdot|x)$  are degenerate.

- **Conditional GAN** uses the following min max loss:

$$\min_{\theta} \max_{\phi} \left[ \underbrace{\mathbb{E}_{x,y \sim \pi^*} \log(D_{\phi}(y|x))}_{\text{Joint, requires pairs } (x,y) \sim \pi^*} + \underbrace{\mathbb{E}_{x \sim \pi_x^*} \mathbb{E}_{z \sim p_z} \log(1 - D_{\phi}(G_{\theta}(z|x)|x))}_{\text{Marginal, requires } x \sim \pi_x^*} \right],$$

where  $G_{\theta} : \mathcal{Z} \times \mathcal{X} \rightarrow \mathcal{Y}$  is the conditional generator with parameters  $\theta$ ,  $p_z$  is a distribution on latent space  $\mathcal{Z}$ , and  $D : \mathcal{Y} \times \mathcal{X} \rightarrow (0, 1)$  is the conditional discriminator with parameters  $\phi$ . From the loss it is clear that the model can use not only paired data during the training, but also samples from  $\pi_x^*$ . The minimum of this loss is achieved when  $G(\cdot|x)$  generates  $\pi^*(\cdot|x)$  from  $p_z$ .

- **Unconditional GAN +  $\ell^2$  loss** optimizes the following min max objective:

$$\min_{\theta} \max_{\phi} \left[ \lambda \underbrace{\mathbb{E}_{(x,y) \sim \pi^*} \mathbb{E}_{z \sim p_z} \|y - G_{\theta}(x,z)\|^2}_{\text{Joint, requires pairs } (x,y) \sim \pi^*} + \underbrace{\mathbb{E}_{y \sim \pi_y^*} \log(D_{\phi}(y))}_{\text{Marginal, requires } y \sim \pi_y^*} + \underbrace{\mathbb{E}_{x \sim \pi_x^*} \mathbb{E}_{z \sim p_z} \log(1 - D_{\phi}(G_{\theta}(x,z)))}_{\text{Marginal, requires } x \sim \pi_x^*} \right],$$

where  $\lambda > 0$  is a hyperparameter. In turn,  $G_{\theta} : \mathcal{X} \times \mathcal{Z} \rightarrow \mathcal{Y}$  is the stochastic generator. Compared to the unconditional case, the main idea here is to use the unconditional discriminator  $D_{\phi} : \mathcal{Y} \rightarrow (0, 1)$ . This allows using unpaired samples from  $\pi_y^*$ . However, using only GAN loss would not allow to use the paired information in any form, this is why the supervised  $\ell^2$  loss is added ( $\lambda = 1$ ).

We note that this model has a trade-off between the target matching loss (GAN loss) and regression loss (which suffers from averaging). Hence, the model is unlikely to learn the true paired data distribution and can be considered a heuristical loss to use both paired and unpaired data. Overall, we consider this baseline as most existing GAN-based solutions (Tripathy et al., 2019, §3.5), (Jin et al., 2019, §3.3), (Yang & Chen, 2020, §C), (Vasluianu et al., 2021, §3) for paired and unpaired data use objectives that are *ideologically* similar to this one.

- **Conditional Normalizing Flow** (Winkler et al., 2019) learns an explicit density model

$$\pi^{\theta}(y|x) = p_z(G_{\theta}^{-1}(y|x)) \left| \frac{\partial G_{\theta}^{-1}(y|x)}{\partial y} \right|$$

via optimizing log-likelihood (8) of the paired data. Here  $G_{\theta} : \mathcal{Z} \times \mathcal{X} \rightarrow \mathcal{Y}$  is the conditional generator function. It is assumed that  $\mathcal{Z} = \mathcal{Y}$  and  $G_{\theta}(\cdot|x)$  is invertible and differentiable. In the implementation, we use the well-celebrated RealNVP neural architecture (Dinh et al., 2017). The optimal values are attached when the generator  $G_{\theta}(\cdot|x)$  indeed generates  $\pi^{\theta}(\cdot|x) = \pi^*(\cdot|x)$ .

The conditional flow is expected to accurately capture the true conditional distributions, provided that the neural architecture is sufficiently expressive and there is an adequate amount of paired data available. However, as mentioned in §3.1, a significant challenge arises in integrating unpaired data into the learning process. For instance, approaches such as those proposed by (Atanov et al., 2019; Izmailov et al., 2020) aim to extend normalizing flows to a semi-supervised context. However, these methods primarily assume that the input conditions  $x$  are discrete, making it difficult to directly apply their frameworks to our continuous case.

### B.2.3 BASELINES FOR SWISS ROLL WITH 16K DATA

In this section, we show the results of training of the baselines on the large amount of both paired (16K) and unpaired (16K) data (Figure 3). Recall that the ground truth  $\pi^*$  is depicted in Figure 2c. We see that given a sufficient amount of training data, Conditional GAN (Figure 3b) nearly succeeds in learning the true conditional distributions  $\pi^*(\cdot|x)$ . The same applies to the conditional normalizing flow (Figure 3a), but its results are slightly worse, presumably due to the limited expressiveness of invertible flow architecture. Regression, as expected fails to learn anything meaningful because of the averaging effect (Figure 3d). In turn, the unconditional GAN+ $\ell^2$  (Figure 3c) nearly succeeds in generating the target data  $\pi_y^*$ , but the learned plan is incorrect because of the averaging effect.



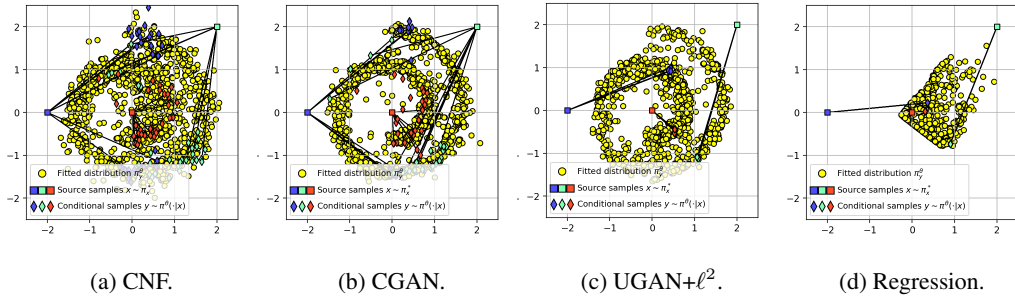


Figure 3: Comparison of the mapping learned by baselines on *Gaussian*  $\rightarrow$  *Swiss Roll* task (§5.1). We use  $P = 16K$  paired data,  $Q = R = 16K$  unpaired data for training.

B.2.4 ABLATION STUDY

In this section, we conduct an ablation study to address the question posed in §3.1 regarding how the number of source and target samples influences the quality of the learned mapping. The results, shown in Figure 4, indicate that the quantity of target points  $R$  has a greater impact than the number of source points  $Q$  (compare Figure 4c with Figure 4b). Additionally, it is evident that the inclusion of unpaired data helps mitigate overfitting, as demonstrated in Figure 4a.

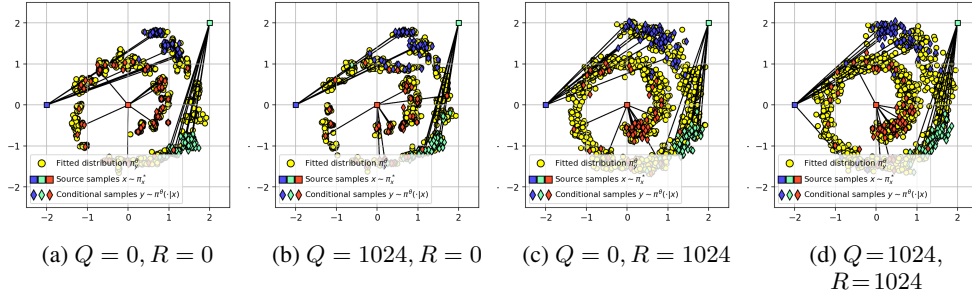


Figure 4: Ablation study analyzing the impact of varying source and target data point quantities on the learned mapping for the *Gaussian*  $\rightarrow$  *Swiss Roll* task (using  $P = 128$  paired samples).

B.3 WEATHER PREDICTION

B.3.1 IMPLEMENTATION DETAILS

In general, we consider the same setting as in B. Specifically, we set  $N = 10, M = 1$  and the number of optimization steps to 30,000. The baseline uses an MLP network with the same number of parameters, predicting the parameters of a mixture of 10 Gaussians.